Original Article

Differential Effect of Acute Iron Overload on Oxidative Status and Antioxidant Content in Regions of Rat Brain

Natacha E. Piloni[1,2], Macarena Reiteri[3], Marcelo P. Hernando[3,4], Claudio O. Cervino[3], and Susana Puntarulo[1,2]

Abstract

The hypothesis of this study is that the cerebral cortex, hippocampus, and striatum of the rat brain are differentially affected in terms of oxidative stress and antioxidant capacity by acute Fe overload because Fe is distributed in a heterogeneous fashion among different regions and cells of the brain. The effects on the lipophilic and hydrophilic cellular environment were compared between regions and with the whole brain. A single dose of Fe-dextran increased Fe deposits, reaching a maximum after 6 hr. Both in whole brain and in cortex region, the ascorbyl/ascorbate content ratio was increased after 6 hr of Fe administration, while in striatum and hippocampus, there was no significant changes after Fe overload. Total thiol content decreased in whole brain and cortex, while there were no significant changes in striatum and hippocampus after Fe overload. The content of α-tocopherol (α-T), whether measured in the whole brain or in the isolated regions, did not change following Fe treatment. Lipid radical (LR$^\bullet$) generation rate after Fe-dextran overload only increased in the cortex region. The LR$^\bullet$/α-T content ratio was increased by Fe treatment in cortex but not in the whole brain, striatum, or hippocampus, in agreement with the study tested hypothesis.

Iron (Fe) is a trace element essential to the maintenance of normal physiological functions. In vertebrates, Fe-containing proteins play a key role in diverse physiological processes, such as oxygen transport, respiration, deoxyribonucleic acid (DNA) synthesis, certain aspects of host defense, xenobiotic metabolism, the synthesis of some essential neurotransmitters and hormones (Gutteridge and Halliwell 2000), and contribute to maintain a necessary "oxidative tone" in neurons (Mura et al. 2006). Yet, because of its ability to undergo 1-electron reactions, Fe^{2+} catalyzes, through the Fenton reaction, the transformation of the mild oxidant hydrogen peroxide (H_2O_2) into hydroxyl radical ($^\bullet OH$), one of the most reactive species in nature (Symons and Gutteridge 1998) that, once generated, reacts with cellular lipids, proteins, and DNA (Gutteridge and Halliwell 2000). On the other hand, animal studies have revealed that feeding rats with low Fe diets early in life results in irreversible alterations of brain functions, which are related to insufficient myelination (Beard and Connor 2003; Ortiz et al. 2004). Thus, although Fe seems to be essential for normal brain function, Fe accumulation is a source of reactive oxygen species (ROS; Hidalgo et al. 2007).

Fe-dextran treatment constitutes a good model for Fe toxicity evaluation, as it leads to similar pathological and clinical consequences observed after acute Fe overload in humans

(Puntarulo 2005). An *in vivo* model consisting of intraperitoneal (ip) Fe-dextran administration, followed by excision of the organ after 6 and 8 hr was characterized in terms of the oxidative status in the liver, kidney, and brain (Galleano and Puntarulo 1992, 1994; Piloni et al. 2013). Piloni et al. (2013) showed the effect of Fe overload by assaying many features of oxidative stress in both the whole brain and different isolated areas. Moreover, catalase (CAT) activity and nuclear factor-kappa B deoxyribonucleic acid (NF-κB DNA)-binding activity were also evaluated. CAT activity was significantly increased after

[1] Facultad de Farmacia y Bioquímica, Fisicoquímica, Universidad de Buenos Aires, Buenos Aires, Argentina
[2] Instituto de Bioquímica y Medicina Molecular (IBIMOL), CONICET-Universidad de Buenos Aires, Buenos Aires, Argentina
[3] Facultad de Ciencias de la Salud, Instituto de Neurociencias-Cátedra de Fisiología, Universidad de Morón, Buenos Aires, Argentina
[4] Depto Radiobiología, Comisión Nacional de Energía Atómica, San Martín, Buenos Aires, Argentina

Corresponding Author:
Susana Puntarulo, Facultad de Farmacia y Bioquímica, Fisicoquímica-IBIMOL, Universidad de Buenos Aires, Buenos Aires, Junín 956, CAAD1113, Buenos Aires, Argentina.
Email: susanap@ffyb.uba.ar

8 hr of Fe administration in cortex, hippocampus, and striatum (1.4-fold, 86%, and 47%, respectively). Fe response in the whole brain seems to lead to an enhancement of NF-κB DNA–binding activity, which was proposed to contribute to limit ROS-dependent damage by triggering the activity of the antioxidant enzyme CAT (Piloni et al. 2013). However, the effect on the nonenzymatic antioxidants was not evaluated yet.

Oxidative stress results from an imbalance between ROS and antioxidants (González et al. 2015). Glutathione (GSH) and its associated enzymes are critical for the degradation of H_2O_2 (Meister and Anderson 1983). GSH is a free radical scavenger and an inhibitor of lipid peroxidation that protects the brain from oxidative stress (Janaky et al. 2007) and contributes to regenerate other antioxidants. Several antioxidants remove ROS and thereby prevent oxidative damage. The enzymatic antioxidants and the nonenzymatic compounds such as hydrophilic (e.g., GSH and ascorbate [AH^-]) and lipophilic (e.g., α-tocopherol, α-T) compounds are critical for the control of oxidative damage (González et al. 2015).

The oxidative reactions are related to the pathogenesis of some neurological diseases, especially with neurodegenerative diseases such as Parkinson's disease (PD) and Alzheimer's disease (AD; Lovell and Markesbery 2007; Zhou, Huang, and Przedborski 2008). It has been hypothesized that Fe could play an etiopathologic role in neurodegenerative diseases such as AD and PD. The first association between Fe and neurodegenerative disease was that found in Hallervorden-Spatz disease, now called neurodegeneration with brain-Fe accumulation (Stankiewicz et al. 2007), an inherited (autosomal recessive) neurodegenerative disease characterized by an early onset of extrapyramidal signs, caused by accumulation of Fe predominantly in the substantia nigra and the globus pallidus (Rosana and La Rosa 2007). More recently, diseases such as neuroferritinopathies and Friedreich's ataxia have been associated with mutations of genes involved in the regulation of Fe metabolism. Furthermore, it has been seen that the Fe content in the brain tends to increase with age, in particular in the sites of the typical lesions of AD and PD (Piñero and Connor 2000). In these diseases, oxidative damage has been found even in early stages of the disease, which would indicate that free radicals are related to the etiology. In addition, oxidative stress caused cellular damage and developed clinical diseases including cardiovascular disease and diabetes (Favier 2006; Halliwell 1994; Newsholme et al. 2007).

The different neural populations that appear in each region of the brain vary in their morphology and biochemical features. Because of this diversity, each neuronal population has a unique molecular composition that determines their vulnerability to oxidative stress (Wang and Michaelis 2010). In the AD, the pyramidal neurons of the hippocampus and cortex are specifically affected; meanwhile in PD, the neurons of the striatum and motor neurons are altered, thus these brain regions were selected for this study on the effect of Fe overload.

The hypothesis of this study is that the selected brain regions of the rat brain are differentially affected in terms of oxidative stress and antioxidant capacity by acute Fe overload. The effects on the lipophilic and hydrophilic cellular environment were compared between selected brain regions and the whole brain.

Materials and Methods

Animal Protocol

The animals, male Sprague-Dawley rats, weighing 180 ± 10 g and aged 45 ± 5 days old, were housed under standard conditions of light, temperature, and humidity with unlimited access to water and food. They were purchased from the animal facility of the School of Pharmacy and Biochemistry of the University of Buenos Aires. Each animal received a single dose of 500 mg/kg body weight of Fe-dextran ip. Control rats were sham-injected ip with saline solution. At specific time points after Fe treatment, brain was removed from the anesthetized animals in a CO_2 chamber. For isolation of cortex, hippocampus, and striatum, brain dissection was performed according to Czerniczyniec et al. (2011). The pieces were rapidly removed and immediately frozen and stored under liquid N_2 until performing the individual assays. The procedures received approval from the Institutional Committee for the Care and Use of Laboratory Animals—School of Pharmacy and Biochemistry (CICUAL-FFyB, RES N°1037), fulfilling the requirements of Guide for the Care and Use of Laboratory Animals (National Academy of Sciences, [NIH] Publication 6-23, revised 1985) and according to the principles and directives of the European Parliament and of the Council (2010/63/EU).

Total Fe Content

Brain samples, dried in an oven at 60°C until constant weight, were mineralized by HNO_3 treatment according to Laurie et al. (1991). Fe content was spectrophotometrically assayed after reduction with thioglycolic acid (8% v/v), measuring the absorbance at $\lambda = 535$ nm in the presence of bathophenanthroline according to Brumby and Massey (1967).

Detection of Lipid Radicals (LR$^\bullet$) Generation Rate by Electron Paramagnetic Resonance (EPR)

LR$^\bullet$ were detected by a spin-trapping technique using N-t-butyl-α-phenyl nitrone (PBN). A 40 mM PBN stock solution was prepared in dimethylsulfoxide (DMSO) immediately prior to use. Brain tissue (25 mg fresh weight [FW]) was homogenized in DMSO-PBN (stock solution), incubated for 30 min, and immediately transferred to a Pasteur pipette for LR$^\bullet$ detection. Instrument settings were as follows: modulation frequency 50 kHz, microwave power 10 mW, microwave frequency 9.75 GHz, centered field 3,487 G, time constant 81.92 ms, modulation amplitude 1.20 G, and sweep width 100,000 G, according to Lai et al. (1986). Quantification of the spin adduct was performed using 2,2,6,6-tetramethylpiperidine-1-oxyl (TEMPO) introduced into the same sample cell used for spin trapping. EPR spectra for both, sample and TEMPO solutions, were recorded at exactly the

same spectrometer settings, and the first derivative EPR spectra were double integrated to obtain the area intensity, then the concentration of spin adduct was calculated according to Kotake et al. (1996).

Detection of Ascorbyl Radical (A•) Content by EPR

Brain tissues were prepared using 25 mg FW/ml in the presence of DMSO to stabilize A• and immediately transferred to a Pasteur pipette for A• detection. The measurements were performed at room temperature in the spectrometer using the following settings: microwave power 10 mW, microwave frequency 9.75 GHz, modulation frequency 500 kHz, centered field 3,520 G, modulation amplitude 1 G, time constant 40.96 ms, and sweep width 15,000 G. TEMPO introduced into the same sample cell used for A• detection was employed for quantification of the spin adduct. The concentration of spin adduct was calculated according to Kotake et al. (1996).

Detection of Ascorbate (AH⁻) Content

Reverse phase High Performance Liquid Cromatography (HPLC) with electrochemical detection was used to assess the content of AH^- (Kutnink et al. 1987). The whole brain samples were homogenized employing 10 mg FW/ml in metaphosphoric acid (MPA; 10% w/v) and centrifuged for 10 min at 12,000 g. The supernatant was filtered through nylon membranes of 0.22 microns. A Supelcosil LC-18 column that was stabilized with MPA mobile phase (0.8% v/v) was used. L-ascorbic acid (Sigma-Aldrich, Buenos Aires, Argentina) was employed as standard.

Determination of α-tocopherol (α-T) Content

Bioanalytical Systems (West Lafayette, IN) LC-4C amperometric detector with a glassy carbon working electrode at an applied oxidation potential of +0.6 V was used for the measurement of the α-T content in homogenates from either the whole brain or the selected brain regions. For the assays, 100 mg of brain tissue was homogenized with 150 μl of 3% (w/v) sodium dodecyl sulfate (SDS), 600 μl of methanol, and 30 μl of butylated hydroxytoluene (BHT) 4% (w/v). Then, α-T was extracted with 500 μl of hexane, and it was evaporated in N_2 (g). Then, the samples were dissolved in 300 μl of ethanol: methanol (1:1), and 20 μl aliquots were injected in the HPLC. Quantification was performed by reverse-phase HPLC with electrochemical detection (Desai 1984). D, L-α-tocopherol (Sigma-Aldrich) was used as standard.

Content of Thiobarbituric Acid Reactive Substances (TBARS)

TBARS content was measured using a modified fluorescence method (Boveris and Puntarulo 1998). An aliquot (50 mg) of brain samples were homogenized with 1 ml of 40 mM potassium phosphate buffer, 120 mM KCl (pH 7.4). To an aliquot of 0.1 ml of homogenate, 0.05 ml of (4% w/v) BHT and 0.25 ml (3% v/v) SDS were added. After mixing, 1 ml of 0.1N HCl, 0.15 ml of (10% w/v) phosphotungstic acid, and 0.5 ml of (0.7% w/v) 2-thiobarbituric acid were added. The mixture was heated for 45 min in boiling water, and TBARS were extracted into 1 ml of n-butanol. After a brief centrifugation, the fluorescence of the butanol layer was measured at $\lambda_{ex} = 515$ nm and $\lambda_{em} = 555$ nm. The values were expressed as nmol TBARS (malondialdehyde equivalents) per milligram of protein. Protein was determined in each experiment as previously described by Lowry et al. (1951), employing 4 μl/ml of the homogenate, using bovine serum albumin as standard fresh protein solution. Malondialdehyde standards were prepared from 1,1,3,3-tetramethoxypropane.

Optical Microscopy (OM)

Brain samples were obtained and fixed for OM immediately after sacrifice. It was used a routine fixation with formalin-buffered solution. Slices were stained with Perls' Prussian Blue and hematoxylin–eosin to detect the presence of Fe deposits in tissues and cellular damage, respectively. For observation and photographs, a Leitz DM2500 optical microscope and a Leica DFC 420 C digital camera (Leica Microsystems, Wetzlar, Germany) were used.

Total Thiols and GSH Content

Total thiols were determined spectrophotometrically in the whole rat brain tissue in the presence of 20 mM EDTA in a concentration of 75 mg/ml, according to Sedlak and Lindsay (1968), employing 5,5-dithiobis(2-nitrobenzoic acid) and measuring absorbance at $\lambda = 412$ nm, using GSH as standard. The standard curve was performed using a 1 mM GSH stock solution. To assess the content of GSH in brain cortex, a reverse phase HPLC with electrochemical detection was used. A Supelcosil LC-18-DB column, which was stabilized with 20 mM NaH_2PO_4, pH 2.7 mobile phase, was used. Samples were homogenated (200 mg/ml) in $HClO_4$ 1 M-EDTA 2 mM, centrifuged at 29,000 g for 20 min at 4°, and 20 μl of the filtered supernatants were diluted 1/20 (v/v) in the mobile phase and injected in the HPLC.

Oxidation Rate of 2′7′-dichlorodihidrofluorescein Diacetate (DCFH-DA)

The oxidation of DCFH-DA was assessed in brain homogenates, according to Malanga, Calmanovici, and Puntarulo (1997). Tissue was homogenized (200 mg/ml) in 100 mM Tris–HCl, pH 7.4, with 2 mM EDTA and 5 mM $MgCl_2$. Then, homogenates were incubated with 980 μl 30 mM 4-(2-hydroxyethyl)-1-piperazinneethanesulfonic acid (HEPES), pH 7.2, 200 mM KCl, 1 mM $MgCl_2$, and 10 μl DCFH-DA (1 mg/ml) diluted in methanol. Samples were incubated for 30 min at 37°C, and fluorescence was determined at $\lambda_{ex} = 488$ nm and $\lambda_{em} = 525$ nm.
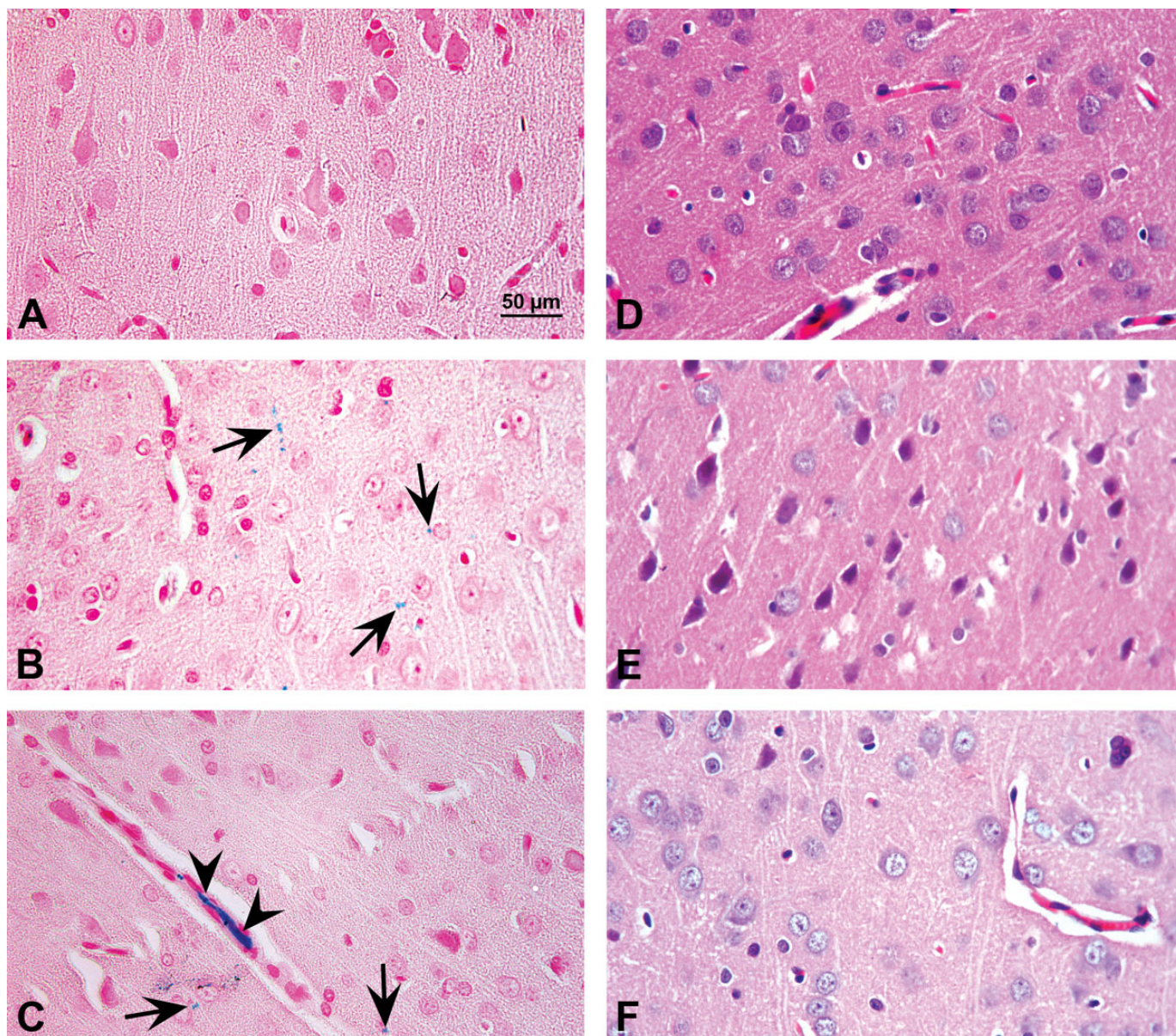
Figure 1. *Upper panel*: Brain section stained with Perls' Prussian blue (original objective 40×) in control and acute Fe-overloaded rats' brain assessed by optical microscopy (OM): (A) brain photomicrograph from a control rat showing normal vasculature and cytoarchitecture, with no Fe deposits; (B) Fe deposits were observed in brain cortical area (arrows) at 6-hr posttreatment (pt); and (C) at 8-hr pt, endothelial (arrow) and vascular (arrow head) Fe deposits was observed in cortex. *Lower panel*: Brain sections were stained with hematoxylin and eosin (original objective 40×) in control and acute Fe-overloaded rats' brain assessed by OM: (D) brain photomicrograph from a control rat shows normal features, (E) at 6-hr pt and, (F) at 8-hr pt a normal cytoarchitecture was observed. Representative images of all brain areas studied.

Statistical Analyses

Unless otherwise indicated, data in the text and tables are expressed as mean ± SEM (standard error of mean) of 3 to 5 independent experiments, with 2 replicates in each experiment. Statistical tests were carried out using Graph InStat; Student *t* test was used to analyze the significance of differences between 2 groups. One-way analysis of variance followed by the New-man–Keuls test was used to analyze the differences between mean values of more than 2 groups. A difference was considered to be statistically significant when $p < .05$.

Results

Tissue Fe was detected by staining brain section with Perls' Prussian Blue, assessed by OM. Control rats showed normal vasculature and cytoarchitecture, and no Fe deposits were observed in cortex (Figure 1a), striatum, and hippocampus (areas not shown). Fe-dextran administration significantly increased Fe deposits in brain cortical area after 6 hr of administration (Figure 1b) and 8-hr posttreatment, and endothelial and vascular Fe deposits were observed in cortex (Figure 1c). Brain cytoarchitecture, assessed by OM, observed by staining
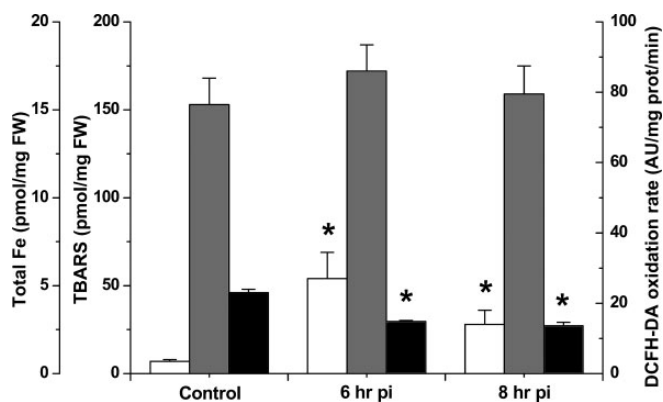
Figure 2. Kinetic study in whole rat brain after acute Fe administration of total Fe content (black), thiobarbituric acid reactive substances (gray), and 2′7′-dichlorodihidrofluorescein diacetate oxidation rate (white). *Significantly different from control values according to Newman–Keuls test after analysis of variance analysis ($p < .05$).

brain section with hematoxylin and eosin, showed normal features (Figure 1d) that were not significantly affected by Fe administration neither 6- (Figure 1e) nor 8-hr (Figure 1f) posttreatment.

Total Fe content upon acute Fe-dextran treatment, assessed after acid mineralization of total rat brain, was significantly increased in brain tissue after 6 hr and 8 hr after Fe administration (Figure 2), with a maximum reached at 6 hr (5.4 ± 1.5 pmol/mg FW), as compared to control values (1.0 ± 0.1 pmol/mg FW), in agreement with the data reported employing OM. TBARS content in whole brain tissue was not affected neither after 6 hr nor 8 hr of Fe-dextran administration (Figure 2). On the other hand, the rate of oxidation of DCFH-DA significantly decreased in brain homogenates from Fe-treated rats (29 ± 1.0 AU/mg protein/min at 6 hr and 8 hr) as compared to values in control whole brains (46 ± 2.0 AU/mg protein/min; Figure 2), suggesting alterations in the oxidative/antioxidant cellular condition.

A typical EPR spectrum for A$^\bullet$ was measured in the whole rat brain homogenates with the following spectral parameters: $g = 2.005$ and $a_H = 1.8$ G (Figure 3, left panel). The content of A$^\bullet$ in Fe-overloaded rat brains was significantly increased after 6 hr of Fe administration and returned to control values 8-hr posttreatment (Figure 3 left panel: d, e). AH$^-$ content in the whole brain was not affected by the Fe overload (0.30 ± 0.02, 0.38 ± 0.02, and 0.28 ± 0.02 nmol/mg tissue, in control, 6- and 8-hr posttreatment, respectively). The A$^\bullet$/AH$^-$ content ratio, understood as an index of oxidative stress in the hydrophilic medium (González et al. 2013), was significantly higher in whole rat brains from control animals as compared to data determined in samples from rats receiving acute Fe-dextran 6
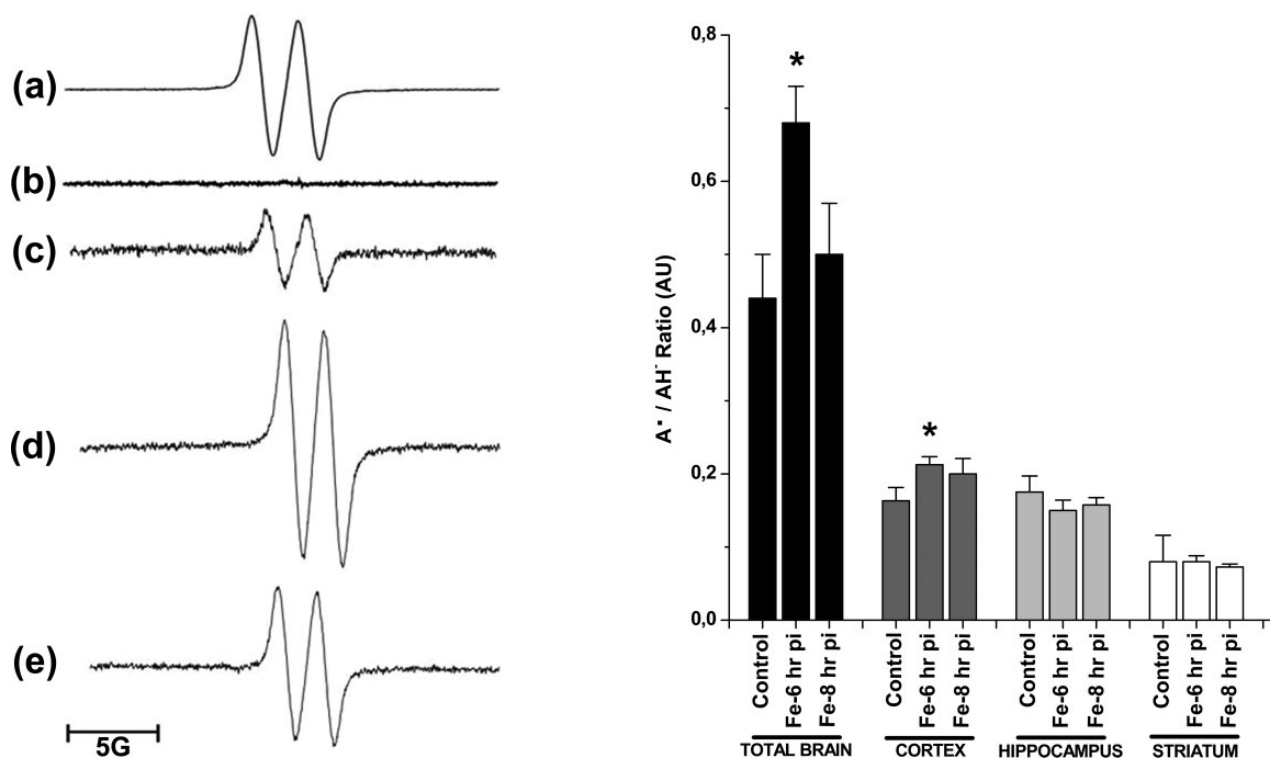
Figure 3. *Left panel*: electron paramagnetic resonance signal for A$^\bullet$ in the whole rat brain homogenates (a) a computer-simulated spectrum employing the following spectral parameters: $g = 2.005$ and $a_H = 1.8$ G, (b) dimethylsulfoxide alone, (c) control rat brain, (d) Fe-overloaded rat brain at 6-hr posttreatment (pt), and (d) at 8-hr pt. *Right panel*: Acute Fe overload effect on the A$^\bullet$/AH$^-$ ratio in whole rat brain, cortex, hippocampus, and striatum after 6- and 8-hr Fe treatment. *Significantly different from control values according to Newman–Keuls test after analysis of variance analysis ($p < .05$).

hr before (Figure 3, right panel). In cortex area from Fe-overloaded rats, the $A^\bullet/AH^-$ ratio was also significantly increased after 6 hr of Fe administration, while in striatum and hippocampus, there were no significant changes over the studied period (Figure 3 right panel).

Total thiols content was significantly decreased in whole brain samples after 6 hr and 8 hr of the Fe-dextran administration as compared to control tissue (Figure 4 upper panel). In cortex area isolated from Fe-overloaded rats, the total thiol content was also significantly decreased after 6 and 8 hr of Fe overload, while in striatum and hippocampus, there were no significant changes over the studied period ($p > .05$; Figure 4 upper panel). Lower panel of Figure 4 shows that GSH content was also significantly decreased in cortex area after 6 hr and 8 hr of Fe overload.

A typical EPR spectrum for $LR^\bullet$ with hyperfine coupling constant $a_H = 1.8$ G, in concordance with computer-simulated signals, was observed after 30 min of incubation of homogenates from cortex of rat brain in combination with the spin trap PBN (Figure 5 A). PBN alone was examined, and no adducts were observed (Figure 5, left panel: b). $LR^\bullet$ generation rate, assessed by quantification of the EPR signals, was not significantly different in the whole brain comparing control with Fe-overloaded brain after 6 hr or 8 hr of Fe-dextran administration (Figure 5, left panel), in agreement with the TBARS data. The same response pattern was observed using either striatum or hippocampus areas of the brain. However, in cortex region, a significant increase in $LR^\bullet$ generation rate was observed in samples after 6 hr of Fe-dextran overload (Figure 5, right panel). The content of the lipid soluble antioxidant α-T was not significantly different between control and overloaded brain samples or selected brain region values (Figure 6 left panel). The $LR^\bullet/\alpha$-T content ratio, considered as an indicator of the balance between free radical damage and antioxidant protection in the hydrophobic medium (Malanga et al. 2009), was not significantly different between control and Fe-dextran overload samples of the whole brain, striatum, or hippocampus regions. However, in the cortex region after 6 hr of Fe-dextran administration, the $LR^\bullet/\alpha$-T content ratio was significantly higher as compared with values in control samples (Figure 6 right panel).

Discussion

The administration of a single dose of Fe dextran was suggested to be a good model for studying Fe-overload toxicity in brain (Piloni et al. 2013). In this work, this model was shown to increase Fe deposits in whole brain, assessed by both microscopy and Fe content measurements, with a maximum reached 6 hr after Fe-dextran administration in agreement with previous results. Moreover, lipid deterioration of the whole brain was not detected after Fe overload, but the oxidation rate of DCFH-DA not only was increased but also was shown to be significantly decreased 6 hr and 8 hr after Fe-dextran single doses. This result opened the question about the complexity of the scenario as compared to the one presented previously. A key
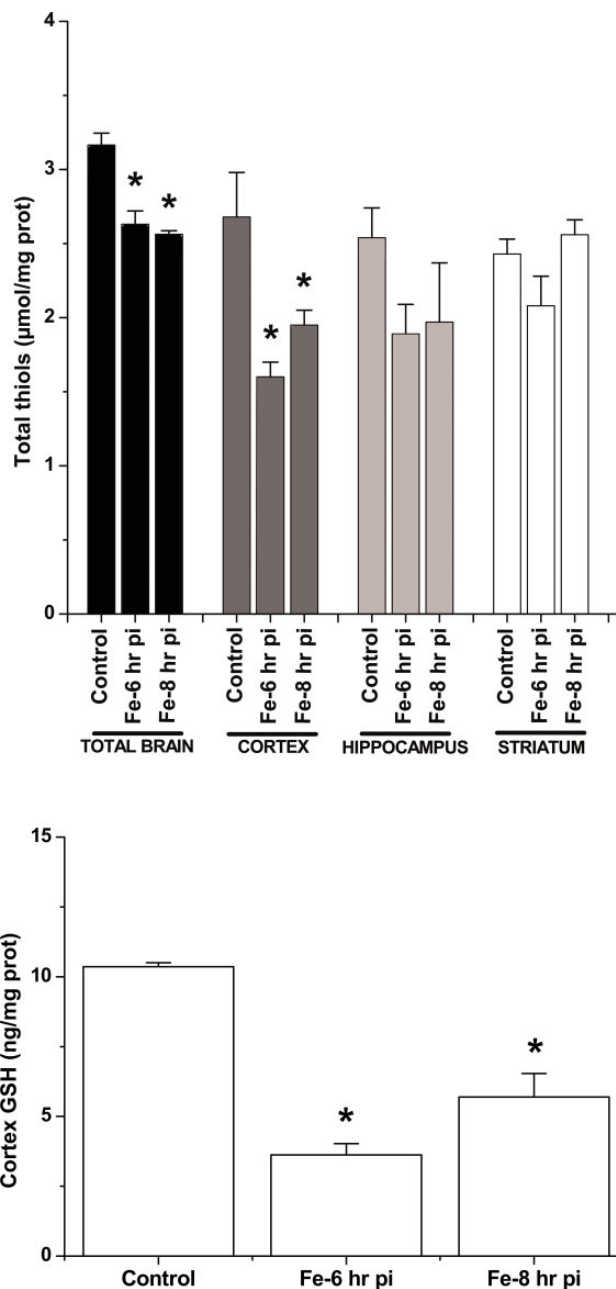

Figure 4. *Upper panel*: Total thiol content in the whole brain and studied areas. *Lower panel*: Cortex glutathione content determined by HPLC from control and Fe-overloaded brains. *Significantly different from control values according to Newman–Keuls test after analysis of variance analysis ($p < .05$).

feature of the brain is the critical role that diversification plays in the organ biological function. Because of its capacity to participate in 1-electron reactions, Fe is a prooxidant element, however, the prooxidant activity of Fe is not necessarily deleterious to neurons and may even be essential if is maintained within physiological limits. The hypothesis presented here was that not all the organ regions are equally able of handling the Fe-derived oxidative alterations in tissues. In this regard, the increase in the $A^\bullet/AH^-$ ratio in the total brain 6 hr after the Fe
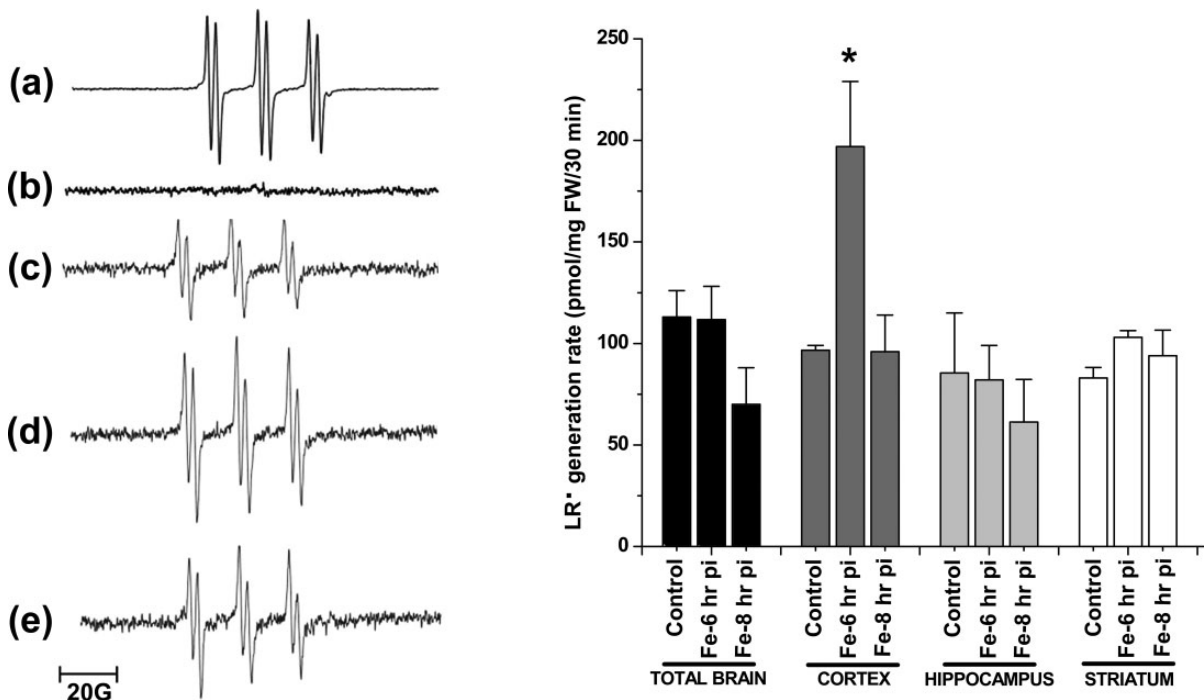
Figure 5. *Left panel*: electron paramagnetic resonance signal for LR$^{\bullet}$ in control and Fe-overloaded rat cortex: (a) computer-simulated spectrum employing the following spectral parameters: $g = 2.005$ and $a_H = 1.8$ G, (b) N-t-butyl-α-phenyl nitrone–dimethylsulfoxide alone, (c) control rat brain, (d) Fe-overloaded rat cortex at 6-hr posttreatment (pt), and (e) at 8-hr pt. *Right panel*: LR$^{\bullet}$ generation rate in whole rat brain, cortex, hippocampus, and striatum after 6- and 8-hr post Fe treatment. *Significantly different from control values according to Newman–Keuls test after analysis of variance analysis ($p < .05$). LR = lipid radical.
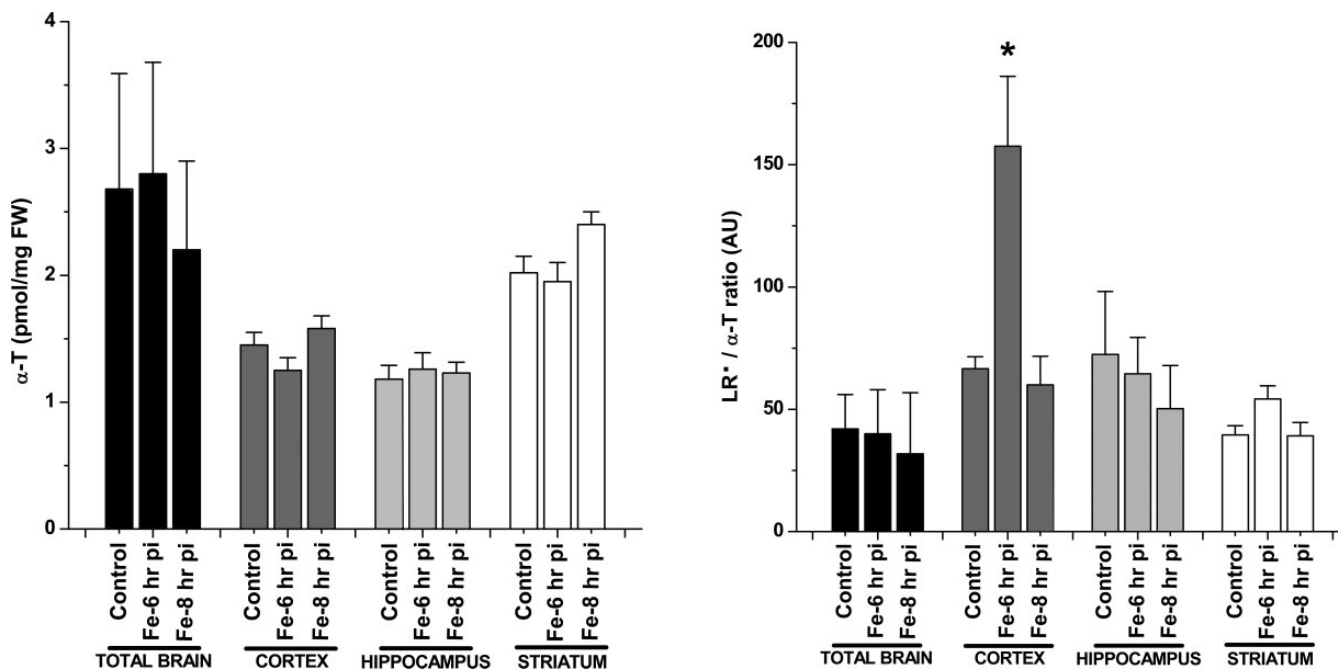
Figure 6. *Left panel*: α-T content in the whole rat brain and the isolated areas after 6- and 8-hr Fe treatment. *Right panel*: kinetic study of LR$^{\bullet}$/α-T ratio in the whole rat brain and the isolated areas after 6- and 8-hr of the Fe treatment. *Significantly different from control values according to Newman–Keuls test after analysis of variance ($p < .05$). LR = lipid radical.

administration seems to mostly reflect the response detected in the cortex region; meanwhile, both hippocampus and striatum regions were not affected. This differential pattern of response could be due to a differential access of Fe to those regions upon Fe administration. However, previous data by Piloni et al. (2013) using this model have shown that Fe content was increased as compared to control values, by 3.4-, 2.6-, and 4.0-fold, respectively, in cortex, hippocampus, and striatum regions, suggesting that this was not the reason of the difference in the oxidative balance in the hydrophilic medium seen after Fe overload. Other possible explanation is that the cortex is, in terms of mass, the major area in the brain as compared to hippocampus and striatum regions; and therefore, the measurements in the whole brain mostly reflect the effects occurring in this region. Nevertheless, a different ability to cope with Fe increase in hippocampus and striatum regions as compared to cortex should not be excluded. Moreover, it is also possible that such effect could be due to a combination of both factors.

The increased $A^\bullet/AH^-$ ratio and the consumption of total thiols in cortex, with no changes in hippocampus and striatum areas reported here, suggested that oxidative balance in the hydrophilic cellular medium was significantly affected by Fe overload and that thiols are an important defense barrier to prevent further damage. These decrease in thiol content seen in the whole brain is again observed in the cortex area and neither in hippocampus nor in the striatum region, suggesting that cortex is more vulnerable than the other studied regions against the increase in Fe content in the studied model. The response, in terms of the decrease in total thiol content in the cortex, is consistent with a similar decrease in the GSH content, reinforcing this observation. Moreover, it has been reported that CAT activity is significantly increased in cortex (2.7-fold) after acute Fe overload, with no changes in hippocampus and striatum regions as compared to the control rats (Piloni et al. 2013). Thus, these results are consistent with the hypothesis that stress imbalance with consumption of some antioxidants (e.g., thiols and GSH) and increase in the activity of others (e.g., CAT) are triggered by Fe overload in the hydrophilic environment of cortex but not in the hippocampus and the striatum regions. It could be postulated that cortex would be more susceptible to oxidative effects than the hippocampus and the striatum regions when exposed to Fe-dextran overload even though Fe content in the striatum and hippocampus was more drastically enhanced than in cortex.

Regarding the oxidative damage in the lipophilic cellular medium after the administration of a single dose of Fe dextran, the $LR^\bullet$ generation rate was not significantly affected, in agreement with the lack of change in the TBARS content, in the whole rat brain, the hippocampus, and the striatum regions. However, the cortex region seems sensitive to Fe-catalyzing effects on lipids 6 hr after Fe-dextran administration in agreement with previous reports from Piloni et al. (2013). The $LR^\bullet/\alpha$-T content ratio was significantly higher from the data obtained in control samples in the cortex region, indicating that oxidative stress plays a role in the lipophilic medium only in the cortex region and that the whole brain does not reflect this

Fe effect. This unexpected result contributes to the complex diversity in the organ not only regarding the selected brain regions but also the phases in the cells that constitute each region. Thus, since vulnerability to oxidative stress differs between brain regions, the strategy to afford clinical therapies should also be different.

Despite the body of evidence that supports the oxidative stress as a pathogenic factor in neurological diseases, the clinical experiences in the use of antioxidants as neuroprotection have been generally negative, mainly with the antioxidants such as AH^- and α-T. However, in the case of animal models of PD and AD, antioxidant therapy has shown more encouraging results (Kamat et al. 2008). On the other hand, several brain permeable Fe chelators have been explored in preclinical models of both diseases but without successful clinical results (Gogoi et al. 2011).

Oxidative stress has been implicated in the pathophysiology of common neurodegenerative disorders (Danysz 2001; Berg and Youdim 2006; Reynolds et al. 2007; Shucla, Mishra, and Pant 2011) such as PD (Méndez-Álvarez et al. 2001; Zhou, Huang, and Przedborski 2008; Nikam et al. 2009), Huntington's disease (Pérez-Severiano et al. 2000; Bogdanov et al. 2001; Stoy et al. 2005), and AD (Behl and Moosmann 2002; Mancuso et al. 2006; Lovell and Markesbery 2007). The markers of oxidative stress were measured in 4 cerebrocortical regions of AD and age-matched control brains (Karelson et al. 2001). The data suggest that in cerebral cortex in AD, the oxidative stress is expressed in the reducing sequence: temporal inferior cortex > frontal inferior cortex > sensory postcentral cortex approximately = occipital primary cortex, corresponding to the histopathological spreading of AD from the associative to primary cortical regions.

Fe accumulation occurs in cortex and hippocampus but not in cerebellum in patients with AD (Duce et al. 2010; Antharam et al. 2012). In addition, Fe accumulation is alone sufficient to cause PD neurodegeneration. Direct Fe injection to rat brains can cause neuron loss (Ben-Shachar and Youdim 1991), and feeding neonatal mice with Fe can trigger later-life parkinsonism and nigral degeneration (Kaur et al. 2007). Oxidative stress plays an important role in the degeneration of dopaminergic neurons in PD (Dias, Eunsung, and Mouradian 2013). Then, the Fe increase observed in neurodegenerative diseases, such as AD and PD, is proposed to be a key mediator in cell loss of these diseases (Ayton, Lei, and Bush 2013; Lei et al. 2012).

O'Donnell (2012) propose that oxidative stress in cortical interneurons may be a final common pathway by which several different etiological factors can yield the cortical dysfunction characteristic of schizophrenia. In addition, oxidative stress has been linked to the neuronal hyperexcitation, and this, to epilepsy seizures (López et al. 2007; Cardenas-Rodriguez et al. 2013).

On the other hand, there is a heterogeneous distribution and accumulation of Fe in the human brain, but the question remains about the reason for these differences between regions of the normal brain. Piñero and Connor (2000) pointed out the

question if the Fe-rich regions are those with high Fe requirement or, rather, regions of low metabolic activity where Fe can be stored in a less oxygen-demanding environment. The latter would require Fe transport to active metabolic regions, a subject that has not been systematically studied.

Taken as a whole, these observations will contribute to the better understanding of the physiological condition of the brain, and the way the unique equilibrium between oxidants and antioxidants is affected by the alteration in the steady state concentration of Fe. However, it the role of Fe in the neurological diseases mentioned before is still not clear. Further studies are required to be able to design therapeutic strategies that would allow to control oxidative damage in specific brain regions to optimize the protocols employed up to now. The assessment of brain-Fe status should be included not only in discussions of diagnosis and treatment of neurological disorders but also in the development of Fe chelators and Fe chelation therapy.

Author Contribution

Authors contributed to conception or design (SP); data acquisition, analysis, or interpretation (NP, MR, MH, CC); drafting the manuscript (NP, SP); and critically revising the manuscript (NP, MR, MH, CC, SP). All authors gave final approval and agreed to be accountable for all aspects of work in ensuring that questions relating to the accuracy or integrity of any part of the work are appropriately investigated and resolved.

Declaration of Conflicting Interests

The author(s) declared no potential conflicts of interest with respect to the research, authorship, and/or publication of this article.

References

Antharam, V., Collingwood, J. F., Bullivant, J. P., Davidson, M. R., Chandra, S., Mikhaylova, A., Finnegan, M. E., et al. (2012). High field magnetic resonance microscopy of the human hippocampus in Alzheimer's disease: Quantitative imaging and correlation with iron. *NeuroImage* **59**, 1249–60.

Ayton, S., Lei, P., and Bush, A. I. (2013). Metallostasis in Alzheimer's disease. *Free Radic Biol* **62**, 76–89.

Beard, J. L., and Connor, J. R. (2003). Iron status and neural functioning. *Annu Rev Nutr* **23**, 41–58.

Behl, C., and Moosmann, B. (2002). Oxidative nerve cell death in Alzheimer's disease and stroke: Antioxidants as neuroprotective compounds. *Biol Chem* **383**, 521–36.

Ben-Shachar, D., and Youdim, M. B. (1991). Intranigral iron injection induces behavioral and biochemical "parkinsonism" in rats. *J Neurochem* **57**, 2133–35.

Berg, D., and Youdim, M. B. (2006). Role of iron in neurodegenerative disorders. *Topics Magn Reson Imaging* **17**, 5–17.

Bogdanov, M. B., Andreassen, O. A., Dedeoglu, A., Ferrante, R. J., and Beal, M. F. (2001). Increased oxidative damage to DNA in a transgenic mouse of Huntington's disease. *J Neurochem* **79**, 1246–49.

Boveris, A. D., and Puntarulo, S. (1998). Free-radical scavenging actions of natural antioxidants. *Nutr Res* **18**, 1545–57.

Brumby, P. E., and Massey, V. (1967). Determination of nonheme iron, total iron and cooper. *Methods Enzymol* **10**, 463–74.

Cardenas-Rodriguez, N., Huerta-Gertrudis, B., Rivera-Espinosa, L., Montesinos-Correa, H., Bandala, C., and Carmona-Aparicio, L. (2013). Role of oxidative stress in refractory epilepsy: Evidence in patients and experimental models. *Int J Mol Sci* **14**, 1455–76.

Czerniczyniec, A., Karadayian, A. G., Bustamante, J., Cutrera, R. A., and Lores-Arnaiz, S. (2011). Paraquat induces behavioral changes and cortical and striatal mitochondrial dysfunction. *Free Radic Biol Med* **51**, 1428–36.

Danysz, W. (2001). Neurotoxicity as a mechanism for neurodegenerative disorders: Basic and clinical aspects. *Expert Opin Investig Drugs* **10**, 985–89.

Desai, I. (1984). Vitamin E analysis methods for animal tissues. *Methods Enzymol* **105**, 138–46.

Dias, V., Eunsung, J., and Mouradian, M. M. (2013). The role of oxidative stress in Parkinson's disease. *J Parkinsons Dis* **3**, 461–91.

Duce, J. A., Tsatsanis, A., Cater, M. A., James, S. A., Robb, E., Wikhe, K., Leong, S. L., et al. (2010). Iron-export ferroxidase activity of β-amyloid precursor protein is inhibited by zinc in Alzheimer's disease. *Cell* **142**, 857–67.

European Union (EU) Directive 2010/63/EU of the European Parliament and of the Council. *OJEU*. Retrieved April 17, 2016.

Favier, A. (2006). Oxidative stress in human diseases. *Ann Pharm Fr* **64**, 390–96.

Galleano, M., and Puntarulo, S. (1992). Hepatic chemiluminescence and lipid peroxidationin mild iron overload. *Toxicology* **76**, 27–38.

Galleano, M., and Puntarulo, S. (1994). Effect of mild iron overload on liver and kidney lipid peroxidation. *Braz J Med Biol Res* **27**, 2349–58.

Gogoi, S., Antonio, T., Rajagopalan, S., Reith, M., Andersen, J., and Dutta, A. K. (2011). Dopamine D_2/D_3 agonists with potent iron chelation, antioxidant and neuroprotective properties: Potential implication in symptomatic and neuroprotective treatment of Parkinson's disease. *Chem Med Chem* **6**, 991–95. doi:10.1002/cmdc.201100140

González, P. M., Aguiar, M. B., Malanga, G., and Puntarulo, S. (2013). Electronic paramagnetic resonance (EPR) for the study of ascorbyl radical and lipid radicals in marine organisms. *Comp Biochem Phys A* **165**, 439–47.

González, P. M., Malanga, G., and Puntarulo, S. (2015). Cellular oxidant/antioxidant network: Update on the environmental effects over marine organisms. *Open Mar Biol J* **9**, 1–13.

Gutteridge, J. M., and Halliwell, B. (2000). Free radicals and antioxidants in the year 2000. A historical look to the future. *Ann NY Acad Sci* **899**, 136–47.

Halliwell, B. (1994). Free radicals, antioxidants, and human disease: Curiosity, cause, or consequence? *Lancet* **344**, 721–24.

Hidalgo, C., Carrasco, M. A., Muñoz, P., and Nuñez, M. T. (2007). A role for reactive oxygen/nitrogen species and iron on neuronal synaptic plasticity. *Antioxid Redox Signal* **9**, 245–55.

Janaky, R., Dohovics, R., Saransaari, P., and Oja, S. S. (2007). Modulation of [3H] dopamine release by glutathione in mouse striatal slices. *Neurochem Res* **32**, 1357–64.

Kamat, C., Gadal, S., Mhatre, M., Williamson, K., Pye, Q., and Hensley, K. (2008). Antioxidants in central nervous system diseases: Preclinical promise and translational challenges. *J Alzheimers Dis* **15**, 473–93.

Karelson, E., Bogdanovic, N., Garlind, A., Winblad, B., Zilmer, K., Kullisaar, T., Vihalemm, T., Kairane, C., and Zilmer, M. (2001). The cerebrocortical areas in normal brain aging and in the Alzheimer's disease: noticeable difference in the lipid peroxidation level and in antioxidant defense. *Neurochem Res* **26**, 353–61.

Kaur, D., Peng, J., Chinta, S. J., Rajagopalan, S., Di Monte, D. A., Cherny, R. A., and Andersen, J. K. (2007). Increased murine neonatal iron intake results in Parkinson-like neurodegeneration with age. *Neurobiol Aging* **28**, 907–13.

Kotake, Y., Tanigawa, T., Tanigawa, M., Ueno, I., Allen, D. R., and Lai, C. S. (1996). Continuous monitoring of cellular nitric oxide generation by spin trapping with an iron dithiocarbamate complex. *Biochim Biophys Acta* **1289**, 362–68.

Kutnink, M. A., Hawkes, W. C., Schaus, E. E., and Omaye, S. T. (1987). An internal standard method for the unattended high-performance liquid chromatographic analysis of ascorbic acid in blood components. *Anal Biochem* **166**, 424–30.

Lai, E. K., Crossley, C., Sridhar, R., Misra, H. P., Janzen, E. G., and McCay, P. B. (1986). In vivo spin trapping of free radicals generated in brain, spleen, and liver during c radiation of mice. *Arch Biochem Biophys* **244**, 156–60.

Laurie, S. H., Tancock, N. P., McGrath, S. P., and Sanders, J. (1991). Influence of complexation on the uptake by plants of iron, manganese, copper and zinc: I. Effect of EDTA in a multimetal and computer simulation study. *Exp Bot* **42**, 509–13.

Lei, P., Ayton, S., Finkelstein, D. I., Spoerri, L., Ciccotosto, G. D., Wrigh, t. D. K., Wong, B. X., et al. (2012). Tau deficiency induces parkinsonism with dementia by impairing APP-mediated iron export. *Nat Med* **18**, 91–95.

López, J., González Fraguela, M. E., Lorigados, L., Morales, L., Riverón, G., and Bauza, J. (2007). Oxidative stress markers in surgically treated patients with refractory epilepsy. *Clin Biochem* **40**, 292–98.

Lovell, M., and Markesbery, W. (2007). Oxidative DNA damage in mild cognitive impairment and late-stage Alzheimer's disease. *Nucleic Acids Res* **35**, 7497–504.

Lowry, O. H., Rosebrough, N. J., Farr, A. L., and Randall, R. J. (1951). Protein measurement with the Folin phenol reagent. *J Biol Chem* **193**, 265–75.

Malanga, G., Calmanovici, G., and Puntarulo, S. (1997). Oxidative damage to chloroplasts from Chlorella vulgaris exposed to ultraviolet-B radiation. *Physiol Plant* **101**, 455–62.

Malanga, G., Perez, A., Calvo, J., and Puntarulo, S. (2009). The effect of seasonality on oxidative metabolism in *Loxechinus albus*. *Mar Biol* **156**, 763–70.

Mancuso, M., Coppede, F., Migliore, L., Siciliano, G., and Murri, L. (2006). Mitochondrial dysfunction, oxidative stress and neurodegeneration. *J Alzheimer's Dis* **10**, 59–73.

Meister, A., and Anderson, M. E. (1983). Glutathione. *Annu Rev Biochem* **52**, 711–60.

Méndez-Álvarez, E., Soto-Otero, R., Hermida-Aeijeiras, A., López-Real, A. M., and Labandeira-García, J. L. (2001). Effects of aluminium and zinc on the oxidative stress caused by 6-hydroxydopamine autoxidation: Relevance for the pathogenesis of Parkinson's disease. *Biochim Biophys Acta* **1586**, 155–68.

Mura, C. V., Delgado, R., Aguirre, P., Bacigalupo, J., and Núñez, M. T. (2006). Quiescence induced by iron challenge protects neuroblastoma cells from oxidative stress. *J Neurochem* **98**, 11–19.

Newsholme, P., Habe, r. E. P., Hirabara, S. M., Rebelato, E. L., Procopio, J., Morgan, D., Oliveira-Emilio, H. C., Carpinelli, A. R., and Curi, R. (2007). Diabetes associated cell stress and dysfunction: Role of mitochondrial and nonmitochondrial ROS production and activity. *J Physiol* **583**, 9–24.

Nikam, S., Nikam, P., Ahaley, S. K., and Sontakke, A. V. (2009). Oxidative stress in Parkinson's disease. *Indian J Clin Biochem* **24**, 98–101.

O'Donnell, P. (2012). Cortical interneurons, immune factors and oxidative stress as early targets for schizophrenia. *Eur J Neurosci* **35**, 1866–70. doi:10.1111/j.1460-9568.2012.08130.x.

Ortiz, E., Pasquini, J. M., Thompson, K., Felt, B., Butkus, G., Beard, J., and Connor, J. R. (2004). Effect of manipulation of iron storage, transport, or availability on myelin composition and brain iron content in three different animal models. *J Neurosci Res* **77**, 681–89.

Pérez-Severiano, F., Rios, C., and Segovia, J. (2000). Striatal oxidative damage parallels the expression of a neurological phenotype in mice transgenic for the mutation of Huntington's disease. *Brain Res* **862**, 234–37.

Piloni, N. E., Fermandez, V., Videla, L. A., and Puntarulo, S. (2013). Acute iron overload and oxidative stress in brain. *Toxicology* **314**, 174–82.

Piñero, D. J., and Connor, J. R. (2000). Iron in the brain: An important contributor in normal and diseased states. *Neuroscientist* **6**, 435–53.

Puntarulo, S. (2005). Iron, oxidative stress and human health. *Mol Aspects Med* **26**, 299–312.

Reynolds, A., Laurie, C., Mosley, R. L., and Gendelman, H. E. (2007). Oxidative stress and the pathogenesis of neurodegenerative disorders. *Int Rev Neurobiol* **82**, 297–325.

Rosana, A., and La Rosa, L. (2007). A case of hereditary haemochromatosis in a patient with extrapyramidal syndrome. *Blood Transfus* **5**, 241–43.

Sedlak, J., and Lindsay, R. H. (1968). Estimation of total, protein-bound, and nonprotein sulfhydryl groups in tissue with Ellman's reagent. *Anal Biochem* **25**, 192–205.

Shucla, V., Mishra, S. K., and Pant, H. C. (2011). Oxidative stress in neurodegeneration. *Adv Pharmacol Sci* **2011**, 572634. doi:10.1155/2011/572634.

Stankiewicz, J., Panter, S. S., Neema, M., Arora, A., Batt, C., and Bakshi, R. (2007). Iron in chronic brain disorders: Imaging and neurotherapeutic implications. *Neurotherapeutics* **4**, 371–86.

Stoy, N., Mackay, G. M., Forrest, C. M., Christofides, J., Egerton, M., Stone, T. W., and Darlington, L. G. (2005). Tryptophan metabolism and oxidative stress in patients with Huntington's disease. *J Neurochem* **93**, 611–23.

Symons, M. C. R., and Gutteridge, J. M. C. (1998). *Free Radicals and Iron: Chemistry, Biology and Medicine*. Oxford University Press, New York.

Wang, X., and Michaelis, E. (2010). Selective neuronal vulnerability to oxidative stress in the brain. *Front Aging Neurosci* **2**, 12.

Zhou, C., Huang, Y., and Przedborski, S. (2008). Oxidative stress in Parkinson's disease: A mechanism of pathogenic and therapeutic significance. *Ann N Y Acad Sci* **1147**, 93–104.